Chinese Chemical Letters 33 (2022) 3705–3708

Contents lists available at ScienceDirect

Chinese Chemical Letters

journal homepage: www.elsevier.com/locate/cclet

Construction of immobilized films photocatalysts with CdS clusters decorated by metal Cd and BiOCl for photocatalytic degradation of tetracycline antibiotics

Jiajia Li[a,b,*], Ziwei Zhao[c], Zhuoning Li[a], Huijuan Yang[d], Shijun Yue[a], Yuping Tang[a,*], Qizhao Wang[b,c,*]

[a] Key Laboratory of Shaanxi Administration of Traditional Chinese Medicine for TCM Compatibility, and State Key Laboratory of Research & Development of Characteristic Qin Medicine Resources (Cultivation), and Shaanxi Key Laboratory of Chinese Medicine Fundamentals and New Drugs Research, and Shaanxi Collaborative Innovation Center of Chinese Medicinal Resources Industrialization, Shaanxi University of Chinese Medicine, Xianyang 712046, China
[b] School of Water and Environment, Chang'an University, Xi'an 710064, China
[c] College of Chemistry and Chemical Engineering, Northwest Normal University, Lanzhou 730070, China
[d] Institute of Advanced Electrochemical Energy School of Materials Science and Engineering, Xi'an University of Technology, and Shaanxi International Joint Research Centre of Surface Technology for Energy Storage Materials, Xi'an 710048, China

ARTICLE INFO

Article history:
Received 5 August 2021
Revised 11 September 2021
Accepted 27 October 2021
Available online 2 November 2021

Keywords:
CdS/Cd-BiOCl immobilized films photocatalyst
Photodegradation mechanism
Environmental remediation
Charge separation
Tetracycline

ABSTRACT

A kind of CdS/Cd-BiOCl immobilized films photocatalyst was prepared. The optical and physicochemical properties of the CdS/Cd-BiOCl photocatalysts were analysed, and the detailed characterization revealed CdS/Cd-BiOCl films photocatalyst with good charge carrier separation effect. The reusabilities and photocatalytic properties of the samples were studied. The 15%CdS/Cd-BiOCl photocatalyst exhibited superior performance in photocatalytic degradation of tetracycline (TC) and favorable stability under visible light irradiation. As for the photodegradation rate of TC, 15%CdS/Cd-BiOCl exhibited an excellent photodegradation activity, which is 4.06 and 9.53 times higher than that of CdS/Cd and BiOCl, respectively. The results showed that dominant active species are $^{\bullet}O_2^-$ and $^{\bullet}OH$ radicals during photodegradation. The charge transfer in Z-scheme CdS/Cd-BiOCl films photocatalyst could synchronously generate conduct band (CB) electrons in BiOCl and valence band (VB) holes in CdS, and metal Cd served as electron mediator. This work can be a reference for the design of film photocatalysts and new insight for photodegradating towards contaminants.

Tetracycline (TC) could be applied in pharmaceutical industry, animal husbandry and agriculture. Tetracycline residue has been frequently found in soil, water, and even food, which could cause a tremendous threat on public health [1,2]. This has resulted in an increasing demand for degrading antibiotics to obtain clean water. Among the numerous pollutant treatment methods, photocatalytic technique is a green and effective way to treat wastewater [3–5]. CdS is a kind of visible-light responsive material (Energy gap $E_g \approx 2.4$ eV) on degrading organic pollutants, because it owns more negative conduct band (CB) than the reduction potential for $O_2/^{\bullet}O_2^-$. Regrettably, CdS is easy to be deactivated because of its high recombination rate and its photocorrosion, which will lead to cadmium ions leakage and contaminate water resources, thus limiting its practical applications. In order to overcome these drawbacks, many strategies have been proposed such as the optimizing synthetic approaches, formating heterojunction materials, doping with noble metals, supporting cocatalysts [6–9].

Among these strategies, the construction of heterojunctions is a suitable strategy to stabilize the structure, promote the carriers' separation and improve the photocatalytic activity of CdS. BiOCl-based heterojunction photocatalysts exhibit a good photocatalytic performance, owing to their low cost, proper band edges and superior stability characters [10–13]. Nevertheless, the drawback of heterojunction photocatalysts is that it would reduce the potential of photoelectrons and holes as well as weaken the ability of redox of photocatalysts [14], so some novel heterojunction system should be developed to solve this contradiction. For multiple heterojunction photocatalytic systems, Z-scheme photocatalysts not only can efficiently improve the separation rate of photogenerated charge carriers, but also maintain relatively higher redox ability [15,16]. Z-

* Corresponding author.
E-mail addresses: ljjzhw2007@163.com (J. Li), yupingtang@sntcm.edu.cn (Y. Tang), qzwang@chd.edu.cn (Q. Wang).

https://doi.org/10.1016/j.cclet.2021.10.080
1001-8417/

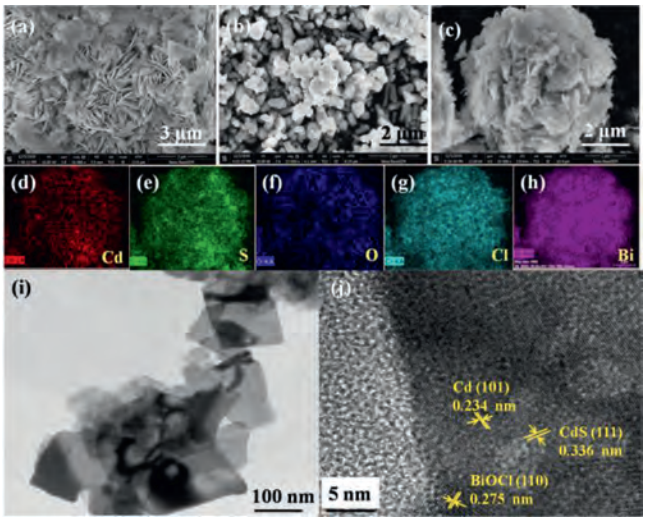

Fig. 1. SEM images of (a) pristine BiOCl, (b) CdS/Cd and (c) CdS/Cd-BiOCl. (d-h) EDX elemental mappings of CdS/Cd-BiOCl. (i) TEM image and (j) HRTEM image of CdS/Cd-BiOCl photocatalysts.

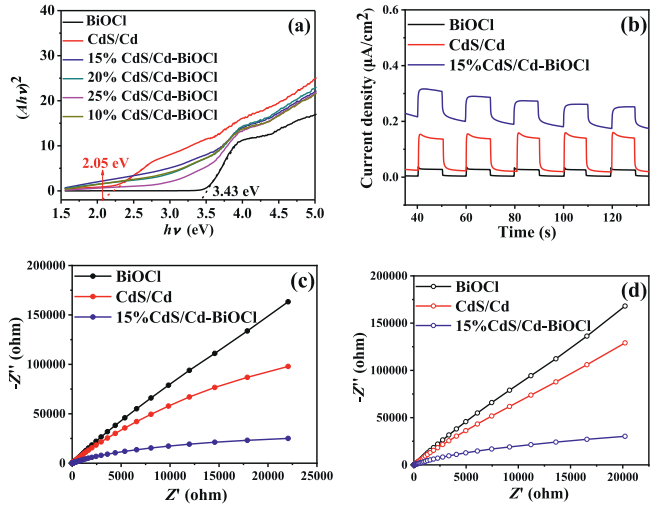

Fig. 2. (a) The band gap evaluation from the plots of $(\alpha h\nu)^2$ *versus* photon energy ($h\nu$). (b) Photocurrent response of the CdS/Cd, BiOCl and 15%CdS/Cd-BiOCl photocatalysts. Nyquist plots of EIS measurements on the CdS/Cd, BiOCl and 15%CdS/Cd-BiOCl electrodes: (c) in the light irradiation and (d) in the dark.

scheme photocatalysts contained two different semiconductor photocatalysts and an electron mediator [17–21]. The most important of Z-scheme system is metal, which can act as electron mediator to decrease the interfacial resistance and facilitate the charge separation. In recent years, non-noble metal Cd has drawn much attention owing to its excellent electrical conductivity and potential applications. Furthermore, Cd and CdS both have the same cadmium element, which leads to their better lattice matching, and previous studies [22–25] have shown that CdS/Cd will be a sort of potential photocatalyst.

Encouraged by the above facts, we attempt to synthesize CdS/Cd-BiOCl Z-scheme film photocatalysts for the removal of tetracycline. The good photocatalytic performance has been derived from this CdS/Cd-BiOCl film photocatalysts due to its good optical property and suitable energy level structure. The preparation of CdS/Cd photocatalyst was similar with the previous work [26]. Bi_2O_3 was added into HCl to obtain BiOCl. Then, adding the as-prepared CdS/Cd powder, the contents of CdS/Cd in CdS/Cd-BiOCl composites depended on the mass fraction of CdS/Cd and Bi_2O_3 powders. The final samples were named as *x*%CdS/Cd-BiOCl, in which *x*% is the mass fraction of CdS/Cd. CdS/Cd-BiOCl powders were added into 1 mL ethanol solution by 30-min sonication. 1 mL suspension was taken by a pipette and sprayed onto a pre-cleaned FTO substrate (Fig. S1 in Supporting information).

The microstructure and morphology of CdS/Cd-BiOCl photocatalysts were observed by EDX elemental mapping, TEM and SEM. In Fig. 1a, the SEM image of BiOCl showed a sheet-like structure. It could be seen that the shape of CdS/Cd samples was nearly spherical and agglomerated (Fig. 1b). Observed from the SEM images as shown in Fig. 1c, CdS/Cd nanoparticles were adhered on the BiOCl surface. The EDX elemental mappings of 15%CdS/Cd-BiOCl were shown in Figs. 1d-h, which indicated the samples contained Cd, S, O, Bi and Cl elements. The obtained composite materials were further investigated by TEM (Fig. 1i), and it showed that CdS/Cd-BiOCl photocatalysts were in sheet-like morphology. The interface between CdS/Cd nanoparticles and BiOCl nanosheets could be observed through the HRTEM image (Fig. 1j). The lattice spacings of 0.275 nm, 0.234 nm and 0.336 nm corresponded to the (110) plane of BiOCl, the (101) plane of Cd and the (111) plane of CdS [21,26]. It indicated that the formation of heterojunction structure between CdS and BiOCl [12], which would be conducive to the transfer of photogenerated charge carriers.

The crystalline structure of as-prepared samples was determined by XRD. However, it was found that XRD patterns of CdS/Cd-BiOCl composites were similar to that of BiOCl (Figs. S2a and b in Supporting information). The CdS/Cd were not obviously detected due to the small amount of CdS/Cd in CdS/Cd-BiOCl. Furthermore, it was discovered that some of these characteristic peaks (Cd, CdS and BiOCl) were close together and overlapped in the XRD spectrum. According to the XPS spectra (Figs. S3a-f in Supporting information), Cd, S, Bi, Cl and O elements [27,28] coexisted in the sample. XPS analyses revealed the coexistence of Cd, CdS and BiOCl in CdS/Cd-BiOCl samples, which was in good agreement with the results from TEM, SEM and XRD.

The optical absorption properties were also investigated for all samples, and the absorption edge of BiOCl is located at about 365 nm (Fig. S4a in Supporting information). Comparatively, CdS/Cd-BiOCl composites owned a wider absorption because of the relatively narrow bandgap of CdS [12]. Hence, the deposition of CdS/Cd on BiOCl broadened the photoabsorption range to the visible-light region, which was vital for superior photocatalytic performance. The bandgaps of CdS/Cd and BiOCl were determined as 2.05 eV and 3.43 eV (*vs.* NHE) respectively, which matched well with the reported results [22,23] (Fig. 2a). With the photodeposition of Cd, the band gap value of CdS/Cd got narrower and the absorption edge of CdS/Cd-BiOCl composites was slightly extended. The probable reason was that the change of the original state of CdS surface, thus it led to the existence of metal Cd and the absence of S atoms, which further increased the formation of dangling bond on CdS surface [22]. Obviously, because of the co-effect of Cd and BiOCl, CdS/Cd-BiOCl composites exhibited enhanced absorption ability, indicating the high-efficiency solar harvesting. The PL emission spectrum (Fig. S4b in Supporting information) of 15%CdS/Cd-BiOCl was similar to that of CdS/Cd with an excitation wavelength of 573 nm, but the intensity was lower, verifying that the photoelectron-hole pairs recombination rate was effectively inhibited. This PL band was due to the deep trap emission in connection with the excess interface sulfur [24,29].

In order to investigate the effort of as-prepared composites on the transport behavior of charge carriers and the response to light on photoelectrodes, photocurrents of CdS/Cd, BiOCl and 15%CdS/Cd-BiOCl were examined, as emerged in Fig. 2b. When the light was turned on, it could be noticed that the photocurrent density was increased swiftly. Nevertheless, when the light was turned

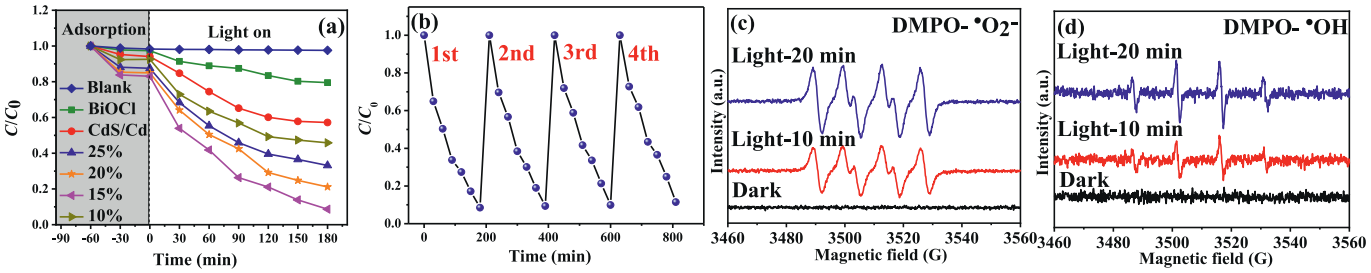

Fig. 3. (a) The photocatalytic activities of various samples toward tetracycline. (b) The photocatalytic cycle tests of sample 15%CdS/Cd-BiOCl. ESR spectra of 15%CdS/Cd-BiOCl for DMPO-$^{\bullet}O_2^-$ (c) and DMPO-$^{\bullet}$OH (d).

off, it was abruptly depressed and maintained a comparative constant value eventually. Strikingly, we learned that the photocurrent density of 15%CdS/Cd-BiOCl attained to 0.3 μA/cm^2, which was 2 and 10 times higher than that of CdS/Cd and BiOCl, respectively. This tendency could be attributed to the efficacious improvement of the charge separation efficiency. At the same time, in order to further investigate the transfer properties of charge carriers, the EIS of the as-synthesized photoelectrodes was evaluated, as presented in Figs. 2c and d. Perspicuously, by contrast with CdS/Cd and BiOCl, 15%CdS/Cd-BiOCl indicated a significant decrement of electrochemical impedance value both in light and dark irradiation conditions. The Nyquist plots delivered the charge-transfer resistance at the surface of the electrode, and the decline of semicircle implied that interfacial charge transfer and the separation of electron-hole pairs [30,31]. Hence, the test data analysis of EIS and PL showed that CdS/Cd-BiOCl could effectively suppress the recombination of photoelectron-hole pairs and accelerate the charge transfer, thereby improving its photocatalytic performance.

Fig. 3a showed the photocatalytic activities of CdS/Cd, BiOCl and a series of CdS/Cd-BiOCl composites. Obviously, there was almost no photodegradation in TC without any photocatalysts. Pure CdS/Cd and BiOCl displayed poor photocatalytic activities, and only 43% and 21% of TC were removed within 3 h of irradiation. It could be found that the photocatalytic activities of the CdS/Cd-BiOCl samples were significantly improved. The TC photodegradation ratios of 10%CdS/Cd-BiOCl, 15%CdS/Cd-BiOCl, 20%CdS/Cd-BiOCl and 25%CdS/Cd-BiOCl reached to 55%, 92%, 79% and 67%, respectively. In particular, 15%CdS/Cd-BiOCl exhibited excellent photocatalytic performance, which was about 2.14 and 4.38 times higher than that of pure CdS/Cd and BiOCl, respectively. The apparent rate constant of photocatalytic degradation of TC over 15%CdS/Cd-BiOCl composite was the highest, which was about 4.06 and 9.53 times higher than that of pure CdS/Cd and pure BiOCl, respectively (Fig. S5a in Supporting information). Further increasing the CdS/Cd loading ($x > 15\%$) leads to the deterioration of photoactivity, which might be ascribed to the surplus CdS/Cd could work as an optical filter to shield incident light and thus the suppressing further enhancement of photocatalytic activity. The recycle experiment of TC removal with the 15%CdS/Cd-BiOCl was performed and the results were shown in Fig. 3b. The degradation efficiency of 15%CdS/Cd-BiOCl showed a slight decrease after four repeated degradations. The slight reduction in the removal performance perhaps could be assigned to the slight loss of photocatalysts during the degradation process. In addition, the results of XRD patterns spectra exhibited a crystal structure of 15%CdS/Cd-BiOCl after the recycling reactions that were consistent with the fresh photocatalyst (Fig. S5b in Supporting information). Therefore, the circulation experiments showed that the construction of CdS/Cd-BiOCl composites could slow down the photocorrosion of CdS.

Moreover, the filtrates of the photodegradation were subjected to the ICP-OES for detecting the leaching of Cd. The obtained results were shown in Table 1. The leached amounts of Cd^{2+} in our work were close to or even less than other reported [32–34]. It could be assumed that the secondary pollution ascribed to leaching made little difference, further indicating that the CdS/Cd-BiOCl composite is a relatively stable photocatalyst.

Table 1
Leached Cd^{2+} after photocatalytic reaction.

Element	Ions leach (%) or concentration (mg/L)	Ref.
Cd^{2+}	1.14%	[32]
Cd^{2+}	4.5×10^{-5} mg/L	[33]
Cd^{2+}	7.17 mg/L	[34]
Cd^{2+}	0.9%	This work

Furthermore, in order to reveal the photocatalytic mechanism over CdS/Cd-BiOCl photocatalysts, we performed the active species capturing experiments. Ammonium oxalate (AO), as a scavenger for h^+, Benzoquinone (BQ) for $^{\bullet}O_2^-$, $AgNO_3$ for e^-, and isopropanol (IPA) for $^{\bullet}$OH, was introduced to the TC solution. The blank experiment demonstrated that the 15%CdS/Cd-BiOCl showed a great performance (Fig. S5c in Supporting information). As an outcome of quenching, with addition of BQ, IPA, $AgNO_3$ and AO separately, TC photodegradation using 15%CdS/Cd-BiOCl photocatalyst was inhibited to different degrees, and the photodegradation removal efficiency at 3 h was decreased to 16.1%, 53.1%, 64.6% and 86.5%, respectively (Figs. S5c and d in Supporting information). Therefore, it revealed that $^{\bullet}O_2^-$ and $^{\bullet}$OH could be the main species in the TC photodegradation process of reaction system. ESR technique was used to detect the presence of various radical species in the dark and under light irradiation. As displayed in Figs. 3c and d, characteristic peaks of DMPO-$^{\bullet}O_2^-$ and DMPO-$^{\bullet}$OH were clearly observed under 10 min of visible light irradiation in 15%CdS/Cd-BiOCl photocatalyst. The results of ESR indicated that $^{\bullet}O_2^-$ and $^{\bullet}$OH species were major active species in this photocatalytic degradation reaction, which was consistent with the results of trapping experiments.

The Mott-Schottky curves of BiOCl and CdS/Cd were investigated (Figs. S6a and b in Supporting information). The positions of CB band for CdS/Cd and BiOCl were –0.41 eV and 0.33 eV respectively. According to the formula of $E_g = E_{VB} - E_{CB}$, the valence band (VB) positions of the CdS/Cd and BiOCl were estimated to be 1.64 eV and 3.76 eV respectively.

As shown in the schematic illustration (Scheme 1), under the visible light irradiation, both BiOCl and CdS are irradiated to generate electron-hole pairs. The work function of Cd (4.08 eV) was lower than that of CdS [22], and the electrons in metallic Cd would transfer to CdS till the Fermi level alignment, which might promote the generation of the active species $^{\bullet}O_2^-$. Meanwhile, after Cd contacting with BiOCl, the CB electrons of BiOCl could readily migrate to the metal Cd and combine with the photoinduced holes in Cd. The VB holes of CdS could be quickly transferred to metal Cd. Therefore, CdS/Cd and BiOCl formed a staggered band position, the CB electrons of BiOCl and the VB holes of CdS were annihi-

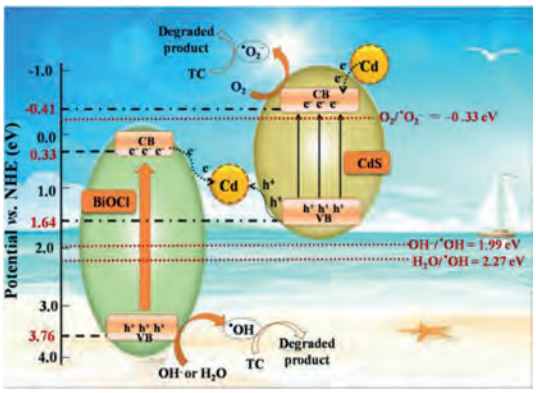

Scheme 1. Schematic illustration of proposed photocatalytic mechanism of CdS/Cd-BiOCl for TC.

lated in metal Cd, resulting in higher electron hole separation rate and redox potential. In addition, the redox potential of $O_2/^{\bullet}O_2^-$ (–0.33 eV) [35] was less negative than the CB of CdS/Cd. Therefore, oxygen could trap the surface electrons of CdS to form $^{\bullet}O_2^-$. Likewise, because the valence band of BiOCl was more positive than the redox potential of $OH^-/^{\bullet}OH$ (+1.99 eV *vs.* NHE) [35] and $H_2O/^{\bullet}OH$ (+2.27 eV *vs.* NHE) [36], h^+ in the BiOCl valence band was easy to capture OH^- and H_2O in the environment and generated a large amount of $^{\bullet}OH$. Consequently, the active species $^{\bullet}O_2^-$ and $^{\bullet}OH$ would attack TC and degrade it. As a result of the differences in band energy potential, a Z-scheme mechanism over the CdS/Cd-BiOCl photocatalysts was proposed. This Z-scheme charge transfer synchronously generated CB electrons in CdS and VB holes in BiOCl, and metal Cd served as electron mediator. It not only endowed the ternary system with superior photoactivity, but also inhibited the photocorrosion of CdS.

In summary, the Z-scheme CdS/Cd-BiOCl films photocatalysts were fabricated, and Cd had been successfully deposited in CdS and acted as an efficient electron mediator. In addition, the 15%CdS/Cd-BiOCl displayed highly efficient photodegradation performance and excellent recycling performance towards TC under simulated solar irradiation. The excellent performance could be attributed to the Z-scheme system, the CB electrons of BiOCl readily migrated to the metal Cd, and the VB holes of CdS could be quickly transferred to metal Cd at the same time, which drastically enhanced the separation efficiency of photoelectron-hole pair. This work may provide a new approach on the rational design of Z-scheme films photocatalysts for photodegradation of organic pollutants, which is of great importance for photocatalysts with efficient charge separation and high photocatalytic performance.

Declaration of competing interest

All authors of this manuscript have directly participated in planning, execution, and/or analysis of this study. The contents of this manuscript have not been copyrighted or published previously. We declare that we have no financial and personal relationships with other people or organizations that can inappropriately influence our work, there is no professional or other personal interest of any nature or kind in any product, service and/or company.

Acknowledgments

This work was also supported by the National Natural Science Foundation of China (Nos. 81573714, 81603258, 81773882 and 21902125), Natural Science Basic Research Program of Shaanxi Provincial Education Department (No. 20JK0607), Young Teacher Research Foundation of Shaanxi University of Chinese Medicine (No. 2020GP33), Subject Innovation Team of Shaanxi University of Chinese Medicine (No. 2019-YL10).

References

[1] L.W. Wang, X.L. Ma, G.F. Huang, et al., J. Environ. Sci. 112 (2022) 59–70.
[2] Z. Cao, Y.F. Jia, Q.Z. Wang, H.F. Cheng, Appl. Clay. Sci. 212 (2021) 106213.
[3] Y. Chen, M.J. Xu, J.Y. Wen, et al., Nat. Sustain. 4 (2021) 618–626.
[4] Q.Y. Yan, C. Lian, K. Huang, et al., Angew. Chem. Int. Ed. 60 (2021) 17155–17163.
[5] M.M. Du, Q.Y. Yi, J.H. Ji, et al., Chin. Chem. Lett. 31 (2020) 2803–2808.
[6] L. Wang, K.Y. Chen, Z.Q. Gao, Q.Z. Wang, Appl. Surf. Sci. 529 (2020) 147217.
[7] F. Ye, H.F. Li, H.T. Yu, et al., Appl. Catal. B: Environ. 227 (2018) 258–265.
[8] S.T. Feng, T. Chen, Z.C. Liu, et al., Sci. Total Environ. 704 (2019) 135404.
[9] Q.Y. Li, Z.P. Guan, D. Wu, et al., J. Am. Chem. Soc. 5 (2017) 6958–6968.
[10] J.X. Wang, Y. Wei, B.J. Yang, et al., J. Catal. 337 (2019) 209–217.
[11] R.R. Jiang, D.H. Wu, G.H. Lu, et al., Chemosphere 227 (2019) 82–92.
[12] J.Q. Zhu, Y.H. Shen, X. Yu, et al., J. Alloys Compd. 771 (2019) 309–316.
[13] J.B. Pan, J.J. Liu, S.L. Zuo, et al., Mater. Res. Bull. 103 (2018) 216–224.
[14] L. Qian, Y.P. Hou, Z.B. Yu, et al., Mol. Catal. 458 (2018) 43–51.
[15] S. Huang, B.F. Zheng, Z.Y. Tang, et al., Chem. Eng. J. 422 (2021) 130086.
[16] S. Patnaik, G. Swain, K.M. Parida, Nanoscale 10 (2018) 5950–5964.
[17] Y.T. Xue, Z.S. Wu, X.F. He, et al., J. Colloid Interface Sci. 548 (2019) 293–302.
[18] C.D. Song, X. Wang, J. Zhang, et al., Appl. Surf. Sci. 425 (2017) 778–795.
[19] S. Bera, S. Ghosh, R.N. Basu, J. Alloys Compd. 830 (2020) 154527.
[20] S. He, C. Yan, X.Z. Chen, et al., Appl. Catal. B: Environ. 276 (2020) 119138.
[21] Q.Y. Li, Z.P. Guan, D. Wu, et al., J. Am. Chem. Soc. 5 (2017) 6958–6968.
[22] W.W. Zhong, S.J. Shen, M. He, et al., Appl. Catal. B: Environ. 258 (2019) 117967.
[23] Q.Z. Wang, J. Hui, J.J. Li, et al., Appl. Surf. Sci. 283 (2013) 577–583.
[24] B. Wang, S. He, W.H. Feng, et al., Appl. Catal. B: Environ. 236 (2018) 233–239.
[25] L. Shang, B. Tong, H.J. Yu, et al., Adv. Energy Mater. 6 (2016) 1501241.
[26] Q.Z. Wang, J.J. Li, Y. Bai, et al., Green Chem. 16 (2014) 2728–2735.
[27] Z.K. Cui, H.T. Song, S.X. Ge, et al., Appl. Surf. Sci. 15 (2019) 505–513.
[28] R.J. Zeng, Z.B. Luo, L.S. Su, et al., Anal. Chem. 91 (2019) 2447–2454.
[29] D.I. Son, D.H. Park, J.B. Kim, et al., J. Phys. Chem. C 115 (2011) 2341–2348.
[30] L. Wang, S.H. Duan, P.X. Jin, et al., Appl. Catal. B: Environ. 239 (2018) 007.
[31] Y.Z. Zhang, S.C. Zong, C. Cheng, et al., Appl. Catal. B: Environ. 233 (2018) 80–87.
[32] M. Darwish, A. Mohammadi, N. Assi, J. Hazard. Mater. 320 (2016) 304–314.
[33] S. Wang, Y. Chen, L.X. Li, et al., Mater. Res. Bull. 99 (2018) 444–452.
[34] G.M. Li, B. Wang, J. Zhang, R. Wang, H.L. Liu, Appl. Surf. Sci. 478 (2019) 1056–1064.
[35] Y.C. Ye, H. Yang, X.X. Wang, et al., Mat. Sci. Semicon. Proc. 82 (2018) 14–24.
[36] G. Lu, F. Wang, X.J. Zou, J. Alloys Compd. 697 (2017) 417–426.